N71-36155

R. A. Summers
Code SR7

17241-6003-R0-00
July 2, 1971

FINAL REPORT

Study of Rocket Experiments to Measure Interplanetary Energetic Hydrogen Fluxes and Hydrogen Fluxes During an Auroral Breakup

Prepared for

NASA HEADQUARTERS
Washington D. C.

Contract NASW-2161

Prepared by:

R. L. Wax

R. L. Wax

Approved by:

A. Rosen

A. Rosen, Director
Space Sciences Laboratory

TRW SYSTEMS
One Space Park
Redondo Beach, Calif. 90278

JAVELIN NEUTRAL HYDROGEN EXPERIMENT

The Javelin rocket, NASA 8:60 CE, was first scheduled for launch on 15 May 1971. However, difficulties with the transmitter caused a postponement until 8 June 1971. While completing final payload assembly at Wallops Island, the H^+ spectrometer channeltron was broken. As a result of consultation with the NASA contract monitor, it was decided that the rocket should not be flown without the H^+ data. Since the repair of the channeltron would have taken at least one week, and since the launch window closed on 15 June 1971, it was decided to reschedule the launch for early January 1972. The Goddard Sounding Rocket Branch was informed and replied that the rescheduling of the launch was feasible and that they would reserve the launch vehicle.

Because of the termination of employment at TRW of W. Bernstein and R. L. Wax, TRW will be unable to complete flight and data reduction of the Javelin rocket. Consequently, the Javelin payload and its associated electronic and mechanical spare parts will be turned over to NASA.

NIKE TOMAHAWK AURORAL HYDROGEN EXPERIMENT

The rocket was launched into a Class III auroral breakup event at 0751 UT, 31 March 1971 from the range at Ft. Churchill. All the data were severely compromised by high voltage corona problems during the flight. The important results include

1. large fluxes of low energy precipitated hydrogen were observed,
2. an H^- component in auroral hydrogen was observed,
3. large amplitude fluctuations in the precipitated low energy electron flux were observed by detectors oriented parallel to the roket spin axis.

A detailed discussion of this flight follows.

NIKE TOMAHAWK FLIGHT

I. LAUNCH CONDITIONS

The vehicle was launched from Ft. Churchill into a Class III auroral breakup at 0151 local time (0751 UT) 31 March 1971. The auroral luminosity (5577) exceeded 120 kR at times and the magnetic bay reached a maximum depression of $\sim 450\gamma$ during the flight. Because the breakup occurred several hours after local magnetic midnight, the breakup pattern moved from west to east. This movement was very striking because general east to west forms were not present in the sky and the major light emission was rather sharply bounded on the eastern border. The vehicle was launched at an 86° elevation and 150° azimuth; it performed well and reached an altitude of ~ 300 Km. The telemetry reception was poor because of many drop-outs probably caused by a poor antenna pattern but was adequate to permit reduction of the data by hand.

II. INSTRUMENTATION

The rocket was instrumented with twelve separate instruments to perform comprehensive measurements of the flux, energy spectra, and pitch angle distributions of precipitated low energy hydrogen (H^o, H^+, and H^-) and electrons, and to identify the occurrence of fast temporal variations in these parameters. Energy range, geometrical factor, resolution, and orientations of these instruments are given in Table I. The swept analyzers were intended to provide details of the particle energy spectra; the fixed energy analyzers were intended to examine rapid temporal variations, pitch angle distributions, and possible transit time delays between the hydrogen and electron precipitation and also between particles of the same type but of different energy.

Thus, the present payload represented a logical extension of the two auroral payloads flown previously [Bernstein et al. 1969, Wax and Bernstein 1970, Bernstein and Wax 1970]; the only "new" instrument included in this flight was the H^- spectrometer [Bernstein et al. 1970] intended to measure the negative ion component in the energetic auroral hydrogen flux.

III. FLIGHT RESULTS

The validity and significance of the flight results are doubtful because of the occurrence of high voltage corona throughout the flight. This resulted in a lowering of the channeltron high voltages as evidenced by the two high voltage monitors. A significantly reduced channeltron high voltage results in an unknown loss of detection efficiency for each individual detector. Since the detectors were intended to operate in the saturated mode, no attempt at efficiency calibration at reduced voltage had been made. In fact, the two high voltage monitors indicated that the high voltage had been reduced to a level where the detectors should have been inoperative throughout the flight. However, all the instruments, with the exception of the electron spectrometer, did count for major periods throughout the flight, and as will be seen, the counting patterns were consistent with ground based optical observations and the expected spin modulation. Therefore we have concluded that the very low voltages indicated by the monitors also were not meaningful, and that the channeltron high voltage was reduced by an unknown and variable factor resulting in unknown and variable efficiencies for each instrument throughout the flight. Comparison of counting rates between different instruments is thus invalid; conclusions relative to long term temporal variations are questionable. The instantaneous energy spectra and observations of short term temporal variations are probably valid but the observed fluxes must be interpreted only in terms of a lower limit to the flux.

The corona and reduced HV problem had been encountered during the vacuum tests at GSFC. At that time, the problem had been solved by the rearrangement and re-potting of the high voltage wires. Two further satisfactory vacuum tests had been performed at GSFC without corona problems and it was concluded that the payload should be flown.

Even during the test at GSFC in which the corona and reduced high voltage problems were present, spurious counts were not observed. Thus we believe that reduced detection efficiency rather than spurious counting rates are the consequence of this malfunction. This conclusion is consistent with the complete absence of counts for all instruments during portions of the flight. This experience with high voltage corona has led to major changes in our assembly of the high voltage portions of the payload of Javelin 8:60 and corona problems have not been encountered during the environmental tests of this payload.

With these shortcomings in mind, we now proceed to the flight data. In Figures 1-5, we present the particle fluxes, corrected for geometrical factor, and resolution, detected by the various operative instruments during the flight. Figure 1 shows the energy channels of the H^o spectrometer, Figure 2 shows the energy channels of the H^- spectrometer, Figure 3 shows the fixed energy electron detectors, Figure 4 shows the fixed energy proton detectors, and Figure 5 shows the ground based optical measurements. Data are absent for periods of variable duration for almost all instruments; during these periods the observed counting rate was not considered significant and probably resulted from a greatly reduced channeltron efficiency. The photometric data are not intended as absolute intensity measurements, and are only intended to show the temporal variations in the emission intensity of the visual aurora in the rocket flight path. Comparison of the relative intensities of the different lines is not valid.

The periods of enhanced optical intensity in the periods 7:53:10 - 7:54:30 and 7:58:24 - 7:58:54 are reasonably well correlated with enhancements in the detected particle fluxes. However, the very large variations observed in the H^- flux in the period 7:56:00 - 7:57:00 are not correlated with any large fluctuations in the optical intensities.

Several selected portions of the fixed energy electron data are presented in Figures 6-8. As can be seen, the detectors oriented at 90° to the rocket spin axis and therefore near 90° to the geomagnetic field lines show the expected spin modulation. However, examples are shown where a much larger modulation at the spin frequency is observed in one of the fixed energy detectors viewing parallel to the spin axis whereas the other parallel detector shows very little modulation. Impulsive variations in the hydrogen and electron fluxes, as observed during our previous flight [Bernstein and Wax 1970], were not observed at any time during the present flight.

IV. DISCUSSION OF RESULTS

A typical precipitated hydrogen energy spectrum derived from the H^{o} spectrometer is shown in Figure 9. The shape of the spectrum does not vary appreciably from 7:54:30 - 7:58:20. During this period, the lower limit to the differential flux can be represented by $dF/dE = 6.5 \times 10^{9} E_{kev}^{-2.7}$ cm^{-2} sec^{-1} kev^{-1} str^{-1}. The present exponent is somewhat smaller than, but consistent with, the values derived in previous flights. The larger flux observed in this flight is consistent with the increased brightness of the aurora. Also shown in Figure 9 is the uncorrected proton energy spectrum and the total hydrogen energy spectrum derived from the proton spectrometer after correction for atmospheric charge exchange and channeltron inefficiency when operated in the saturated mode for protons with energy less than 1 kev. As can be seen from Figure 9, the absolute agreement between the two total hydrogen energy spectra is remarkably good when our lack of knowledge of the absolute detection efficiencies of the two instruments is considered. Once again we conclude that large fluxes of low energy hydrogen are precipitated during the breakup phase. It also appears that at energies at least as low as 100 ev the power law behavior of the total hydrogen spectrum is maintained.

The flux and energy spectra derived from the H^{-} analyzer are not consistent with those derived from the H^{+} analyzer; the H^{-} spectrum shows a pronounced peak in the energy range 1.8 - 2.6 kev. In view of the uncertainty of instrumental efficiencies, this discrepancy in the observed fluxes is not surprising. However, this probably does not account for the discrepancy in spectral shape. As can be seen from Table I, the H^{-} detector always viewed the downward hemisphere at angles near 110° to the rocket spin axis. The proton spectrometer viewed the upward hemisphere at angles near 0° to the spin axis. Therefore the two instruments did not examine the same class of particles, and the observed differences in spectral shape could indeed be valid.

An ∿20 sec period variation in the flux observed in the 1.8 and 2.6 kev channels of the H^- spectrometer is reasonably obvious in Figure 2. This variation is not seen in the "0" volt channel, nor is it evident in the data from the H^+ and H^o spectrometers. Also, spin modulation of the H^- counting rates is not observed although the instrument field of view covered a reasonable range of pitch angles not far removed from 90°. At the present time, we cannot clearly explain the relatively high counting rates observed in the "0" energy channel. Since the correlation between the flux patterns observed in the 1.8 and 2.6 kev channels shows little correlation with that observed in the "0" energy channel, it is difficult to attribute the counts observed in the 1.8 and 2.6 kev channels to any spurious effects. Although we had hoped to obtain a more certain measurement of the H^- flux, we feel that a valid detection of an H^- component in the energetic auroral hydrogen flux has been accomplished.

The large oscillations at the spin frequency observed for a small range of electron energies with the detectors oriented parallel to the spin axis has been observed previously. Figure 10 shows the data from three of the energy channels of the parallel-oriented electron spectrometer from the 1969 flight. Very large modulations are observed for channel 4 electrons ($\sim$4 kev); the spin frequency was 0.7 Hz for the 1969 flight rather than $\sim$6 Hz as in the present flight. The modulation amplitude decreases with decreasing electron energy. In the previous flights, we had attributed the relatively minor spin frequency modulation in the H^+ and H^o detectors to imprecise alignment of the instrument appertures so that a range of pitch angles near 0° would be scanned during each spin cycle. In the case of the electrons however, the modulation depth can exceed a factor of 50; if these results are to be produced simply by poor alignment, a component of the electron pitch angle distribution must be extremely peaked along the lines of force.

REFERENCES

1. Bernstein, W., R. L. Wax and G. T. Inouye, Final Report, Auroral Rocket Experiment II, Contract NASW-1819, 1970.

2. Bernstein, W., G. T. Inouye, N. L. Sanders, and R. L. Wax, "Measurements of Precipitated 1-20 kev Protons and Electrons during an Auroral Breakup", J. Geophys. Res., 74, 3601, 1969.

3. Wax, R. L. and W. Bernstein, "Rocket Borne Measurements of H_β Emissions and Energetic Hydrogen Fluxes during an Auroral Breakup", J. Geophys. Res., 75, 783, 1970.

4. Bernstein, W. and R. L. Wax, "Impulsive Precipitation Events during an Auroral Breakup", J. Geophys. Res., 75, 3915, 1970.

TABLE I

Instrument	Energy Range	Pitch Angles Observed	Geometric Factor (cm^2 str)	Energy Resolution (%)
Negative Hydrogen Analyzer	0-2 kev in 5 steps every 3 seconds	$\sim 110 \pm 14°$	0.10	16
Neutral Hydrogen Analyzer	0-2 kev in 5 steps every 3 seconds	$\sim 0°$	4.2×10^{-2}	37
Proton Analyzer	0-10 kev in continuous sweep every 0.08 sec	$\sim 0°$	2.8×10^{-3}	8.5
Electron Analyzer	0-10 kev in continuous sweep every 0.08 sec	$\sim 0°$	2.5×10^{-4}	8.5
Fixed Proton $H_1 \uparrow$	1.1 kev fixed energy	$\sim 0°$	4.6×10^{-4}	12
Fixed Proton $H_1 \rightarrow$	1.1 kev fixed energy	$\sim 90 \pm 14°$	4.6×10^{-4}	12
Fixed Proton $H_2 \uparrow$	2.2 kev fixed energy	$\sim 0°$	4.6×10^{-4}	12
Fixed Proton $H_2 \rightarrow$	2.2 kev fixed energy	$\sim 90 \pm 14°$	1.75×10^{-3}	12
Fixed Electron $e_1 \uparrow$	1.1 kev fixed energy	$\sim 0°$	4.6×10^{-4}	12
Fixed Electron $e_1 \rightarrow$	1.1 kev fixed energy	$\sim 90 \pm 14°$	4.6×10^{-4}	12
Fixed Electron $e_2 \uparrow$	2.2 kev fixed energy	$\sim 0°$	4.6×10^{-4}	12
Fixed Electron $e_2 \rightarrow$	2.2 kev fixed energy	$\sim 90 \pm 14°$	4.6×10^{-4}	12

FIGURE CAPTIONS

1. Temporal behavior of the fluxes measured in the four energy channels of the H^o spectrometer.

2. Temporal behavior of the fluxes observed with the H^- spectrometer. The "0" energy channel has zero volts applied across the analyzer plates. The counting rate measured in this channel is given in arbitrary units and is presented to show its temporal dependence only.

3. Temporal behavior of the electron fluxes observed with the 1 and 2 kev parallel and perpendicular fixed energy electron detectors.

4. Temporal behavior of the proton fluxes observed with the 1 and 2 kev parallel and perpendicular fixed energy proton detectors.

5. Temporal behavior of the 5577, 3914, and 6300Å light intensity observed with ground based photometers.

6 - 8. Selected examples of variations at the spin frequency observed with the 1 and 2 kev parallel and perpendicular fixed energy electron detectors. Also shown is one axis of the aspect magnetometer.

9. Differential energy spectra of the hydrogen precipitation. The x's denote proton fluxes corrected to top of atmosphere and by channeltron efficiencies. The boxes are the insitu measurements of the protons without correction. The circles represent the insitu atomic hydrogen fluxes.

10. Example of variations at the spin frequency in the electron flux observed with the detector oriented parallel to the spin axis during the 1969 rocket flight.

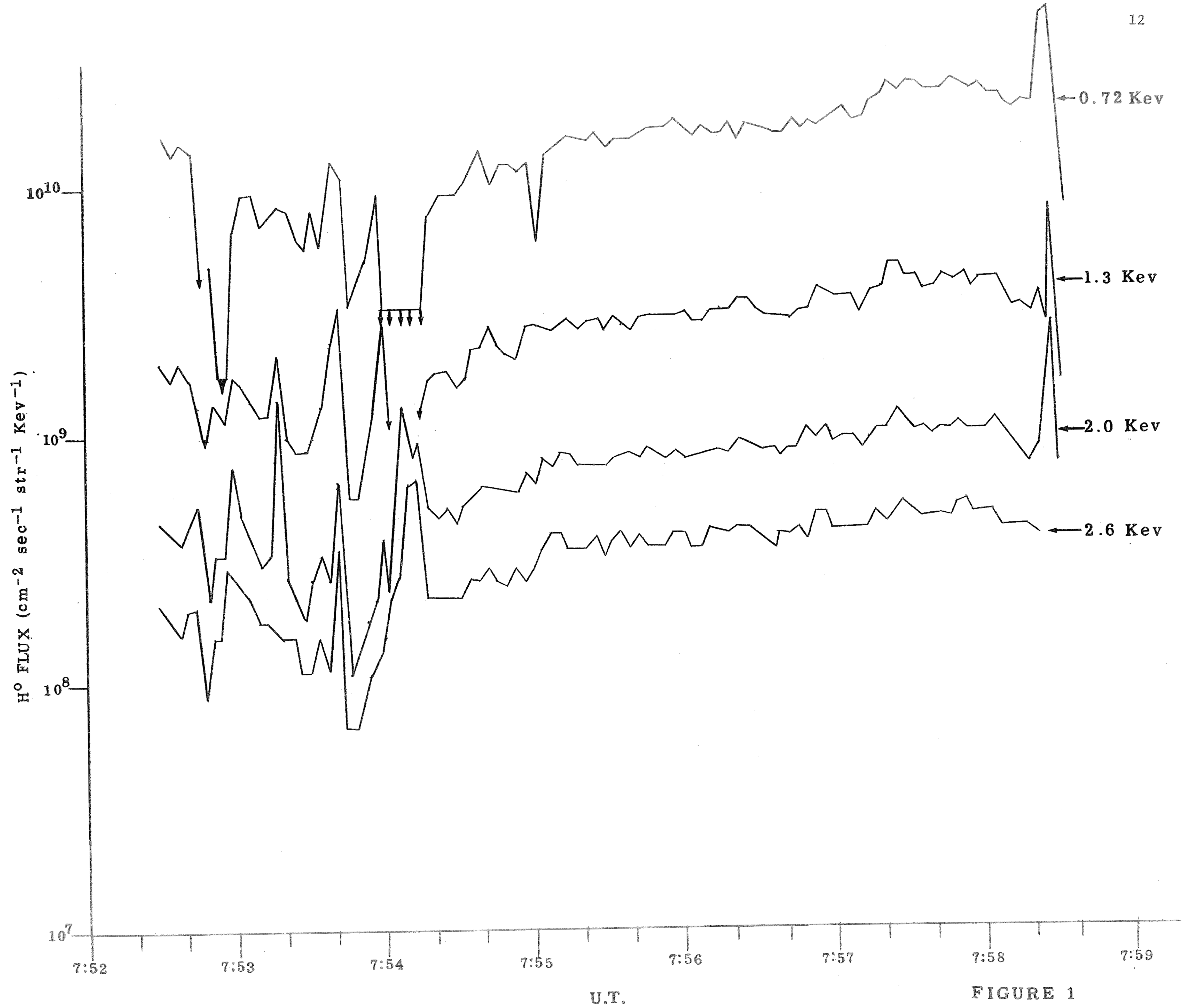
0.72 Kev
1.3 Kev
2.0 Kev
2.6 Kev
10^{10}
10^{9}
10^{8}
10^{7}
H^{o} FLUX (cm^{-2} sec^{-1} str^{-1} Kev^{-1})
7:52
7:53
7:54
7:55
7:56
7:57
7:58
7:59
U.T.

FIGURE 1

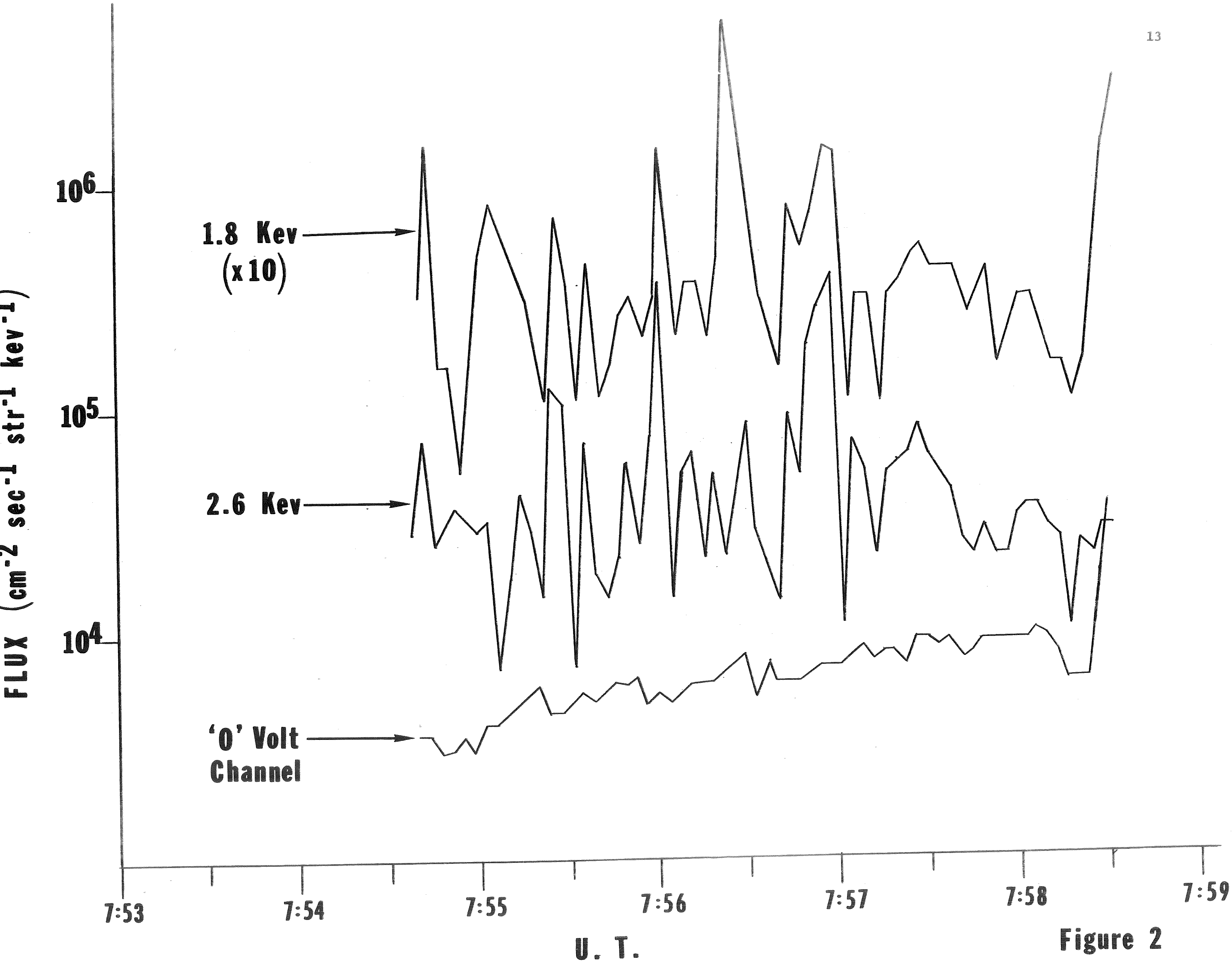

FLUX (cm-2 sec-1 str-1 kev-1)
10^6
10^5
10^4
1.8 Kev (x10)
2.6 Kev
'O' Volt Channel
7:53
7:54
7:55
7:56
7:57
7:58
7:59
U. T.

Figure 2

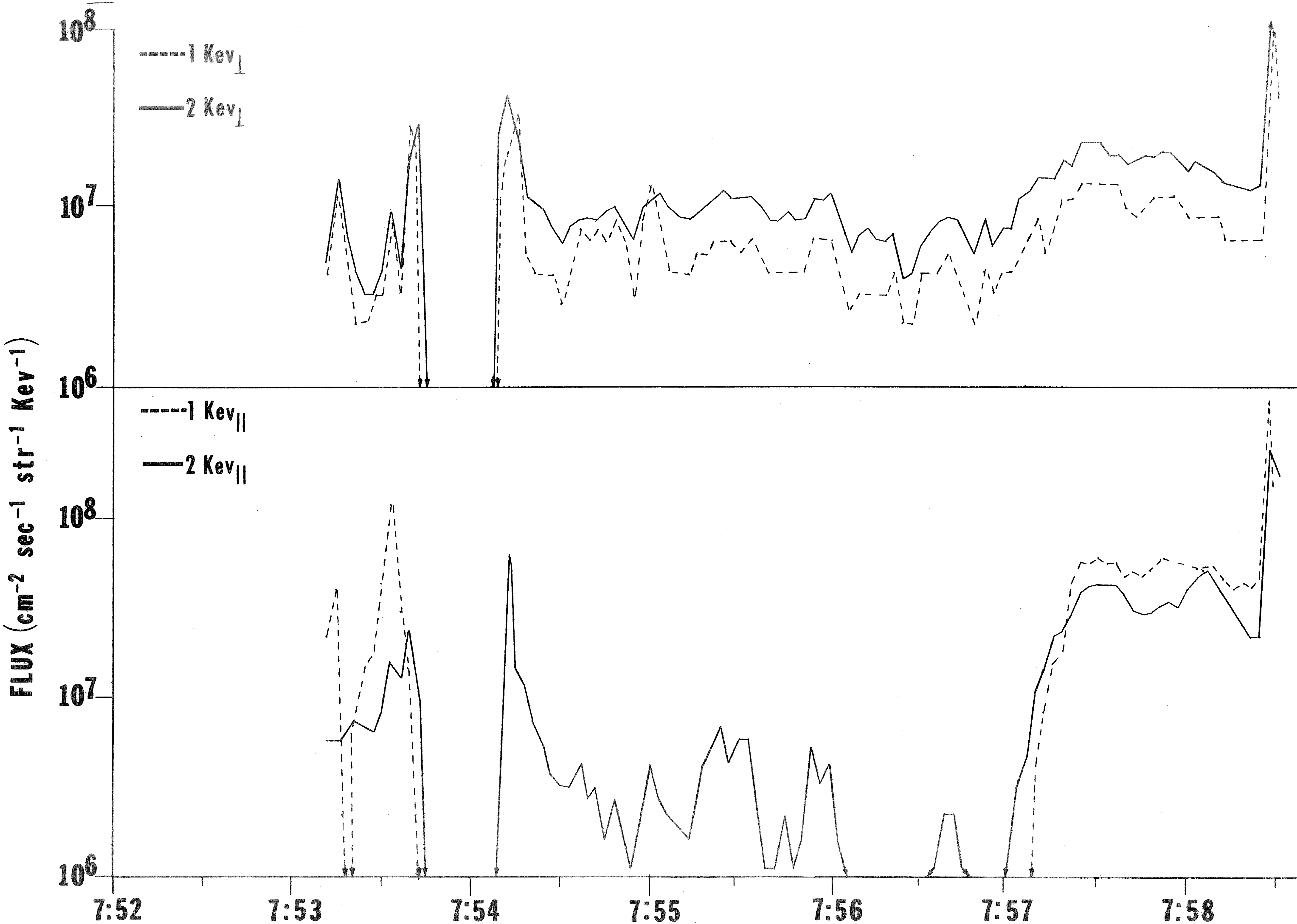

10^8
-----1 Kev$_\perp$
——2 Kev$_\perp$
10^7
10^6
-----1 Kev$_{||}$
——2 Kev$_{||}$
10^8
10^7
10^6
FLUX (cm^{-2} sec^{-1} str^{-1} Kev^{-1})
7:52
7:53
7:54
7:55
7:56
7:57
7:58
U. T.

Figure 3

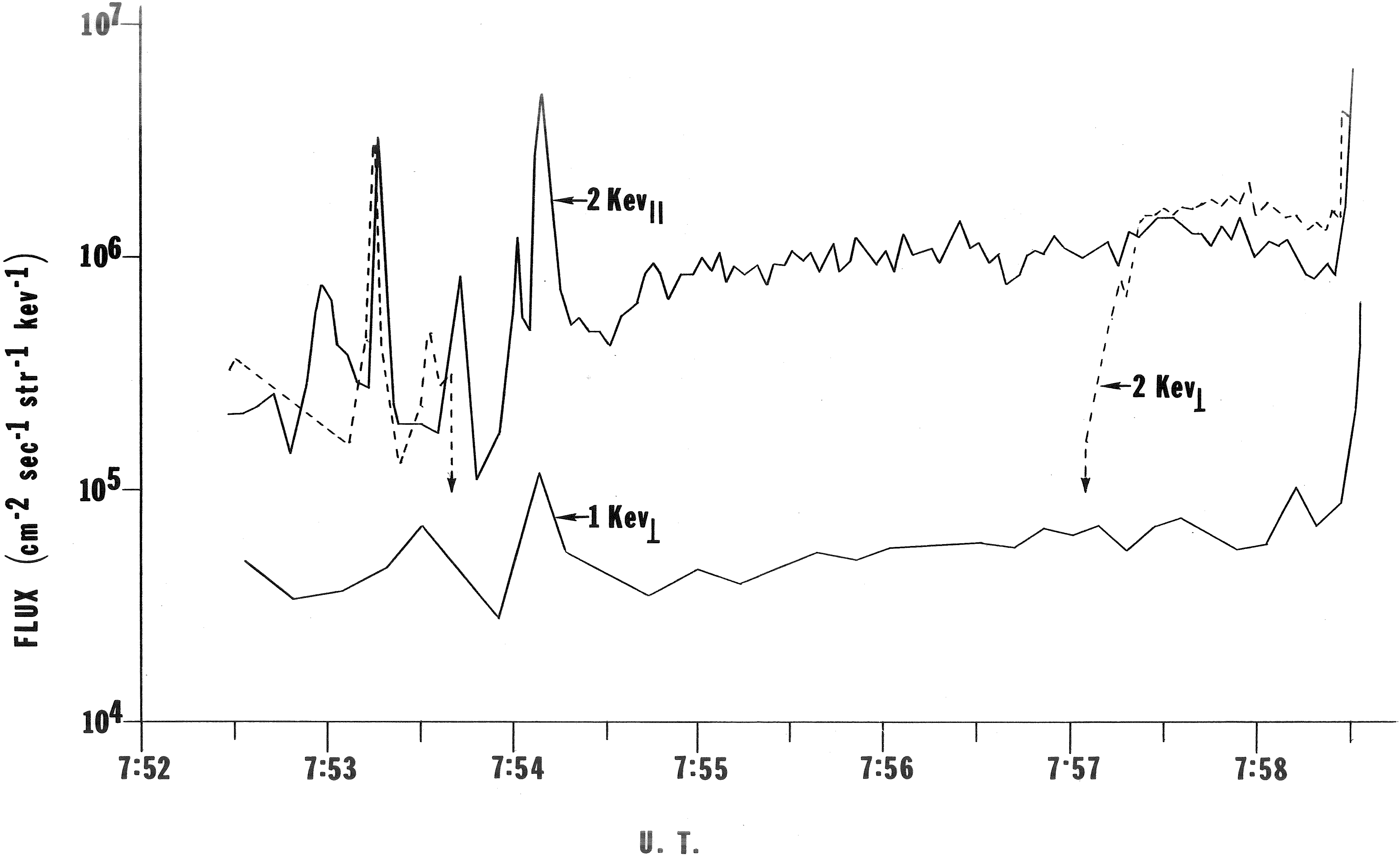

10^7
10^6
10^5
10^4
FLUX $(\mathrm{cm^{-2}\ sec^{-1}\ str^{-1}\ kev^{-1}})$
2 $\mathrm{Kev}_{\parallel}$
2 $\mathrm{Kev}_{\perp}$
1 $\mathrm{Kev}_{\perp}$
7:52
7:53
7:54
7:55
7:56
7:57
7:58
U. T.

Figure 4

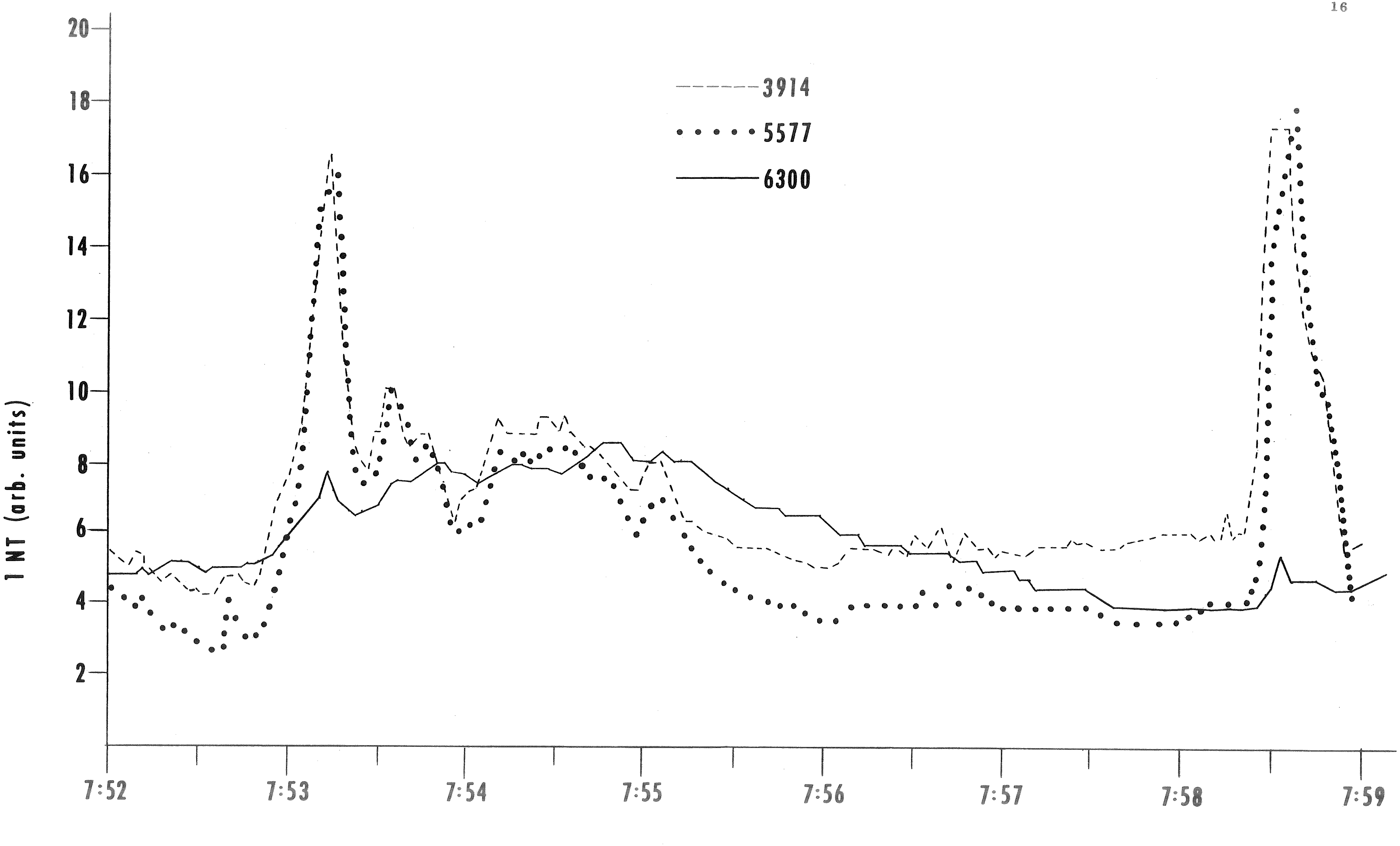
20
18
16
14
12
10
8
6
4
2
I NT (arb. units)
3914
5577
6300
7:52
7:53
7:54
7:55
7:56
7:57
7:58
7:59
U. T.

Figure 5

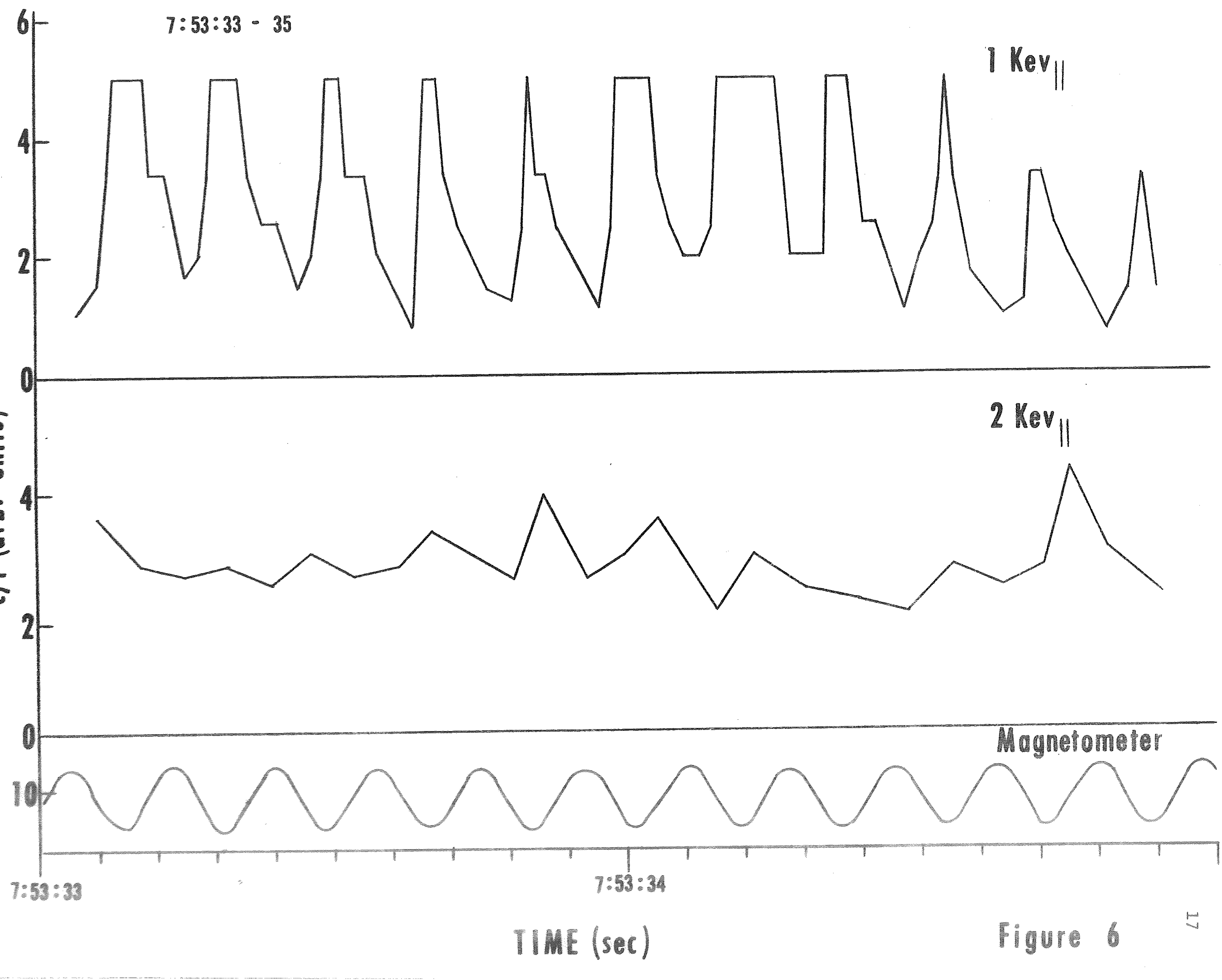
7:53:33 - 35
1 Kev||
2 Kev||
Magnetometer
c/t (arb. units)
6
4
2
0
4
2
0
10γ
7:53:33
7:53:34
TIME (sec)

Figure 6

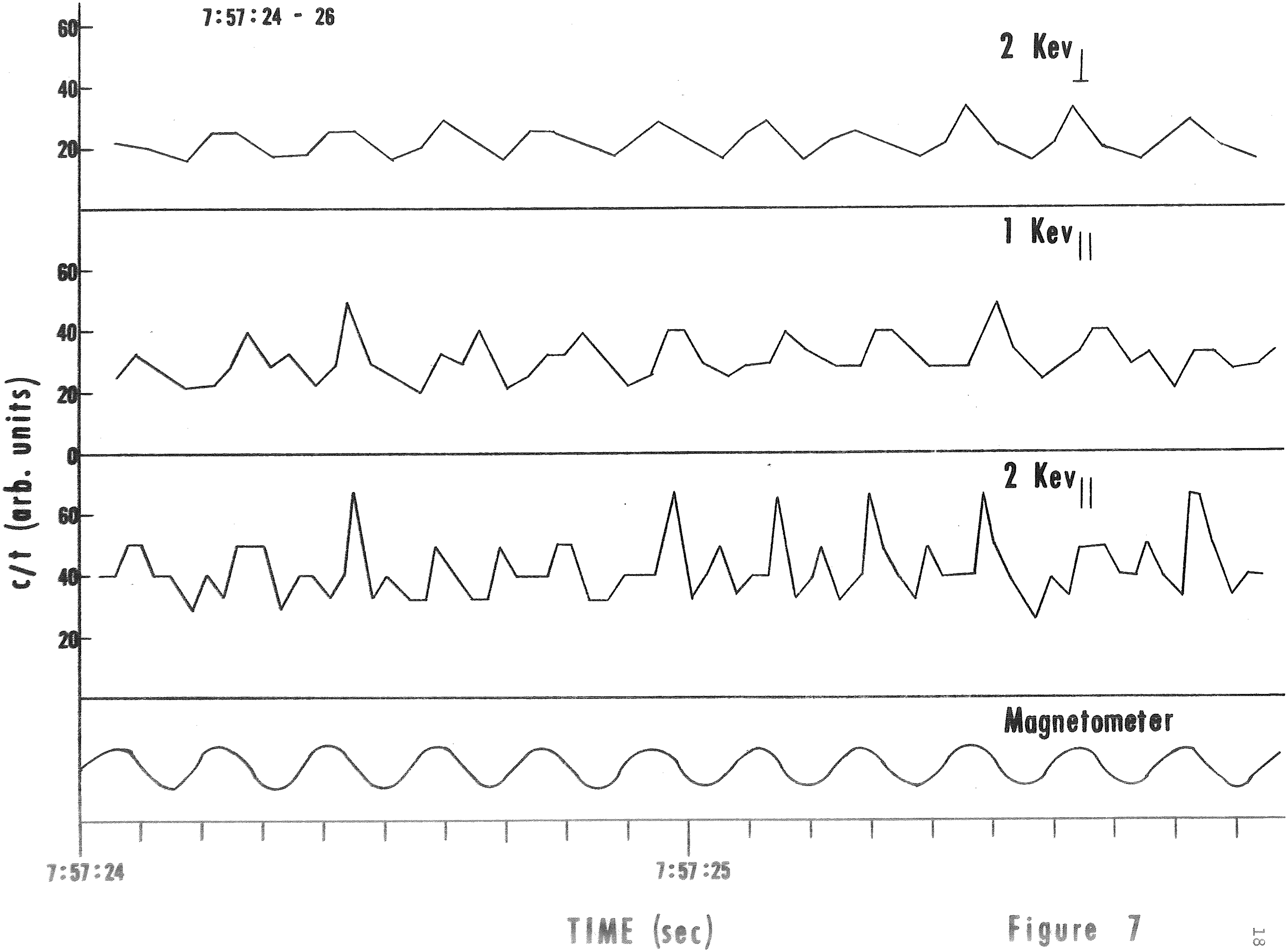

7:57:24 - 26
2 Kev $\perp$
1 Kev $\parallel$
2 Kev $\parallel$
Magnetometer
c/t (arb. units)
60
40
20
0
7:57:24
7:57:25
TIME (sec)

Figure 7

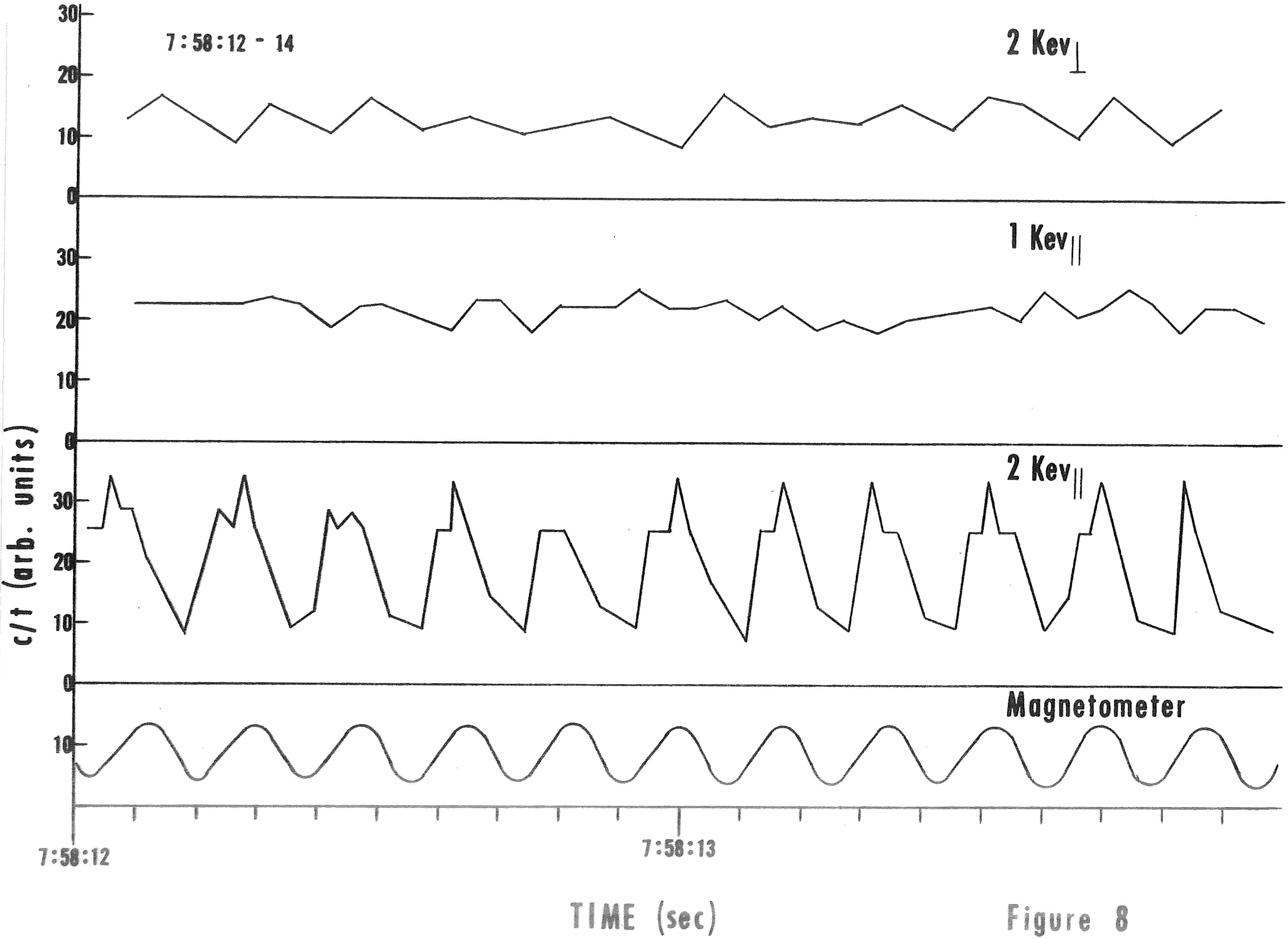
7:58:12 - 14
2 Kev⊥
1 Kev||
2 Kev||
Magnetometer
c/t (arb. units)
30
20
10
0
7:58:12
7:58:13
TIME (sec)

Figure 8

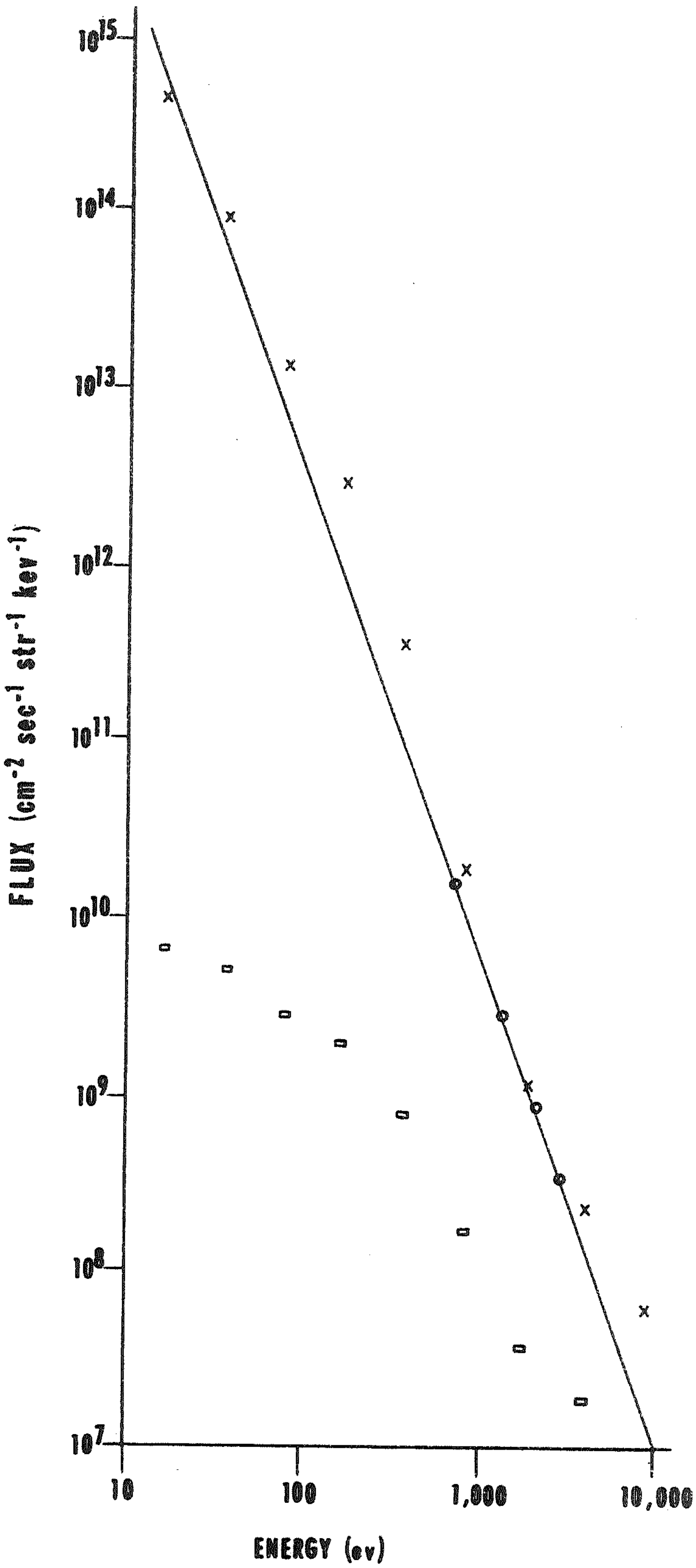

10^{15}
10^{14}
10^{13}
10^{12}
10^{11}
10^{10}
10^{9}
10^{8}
10^{7}
FLUX (cm^{-2} sec^{-1} str^{-1} kev^{-1})
10
100
1,000
10,000
ENERGY (ev)

Figure 9

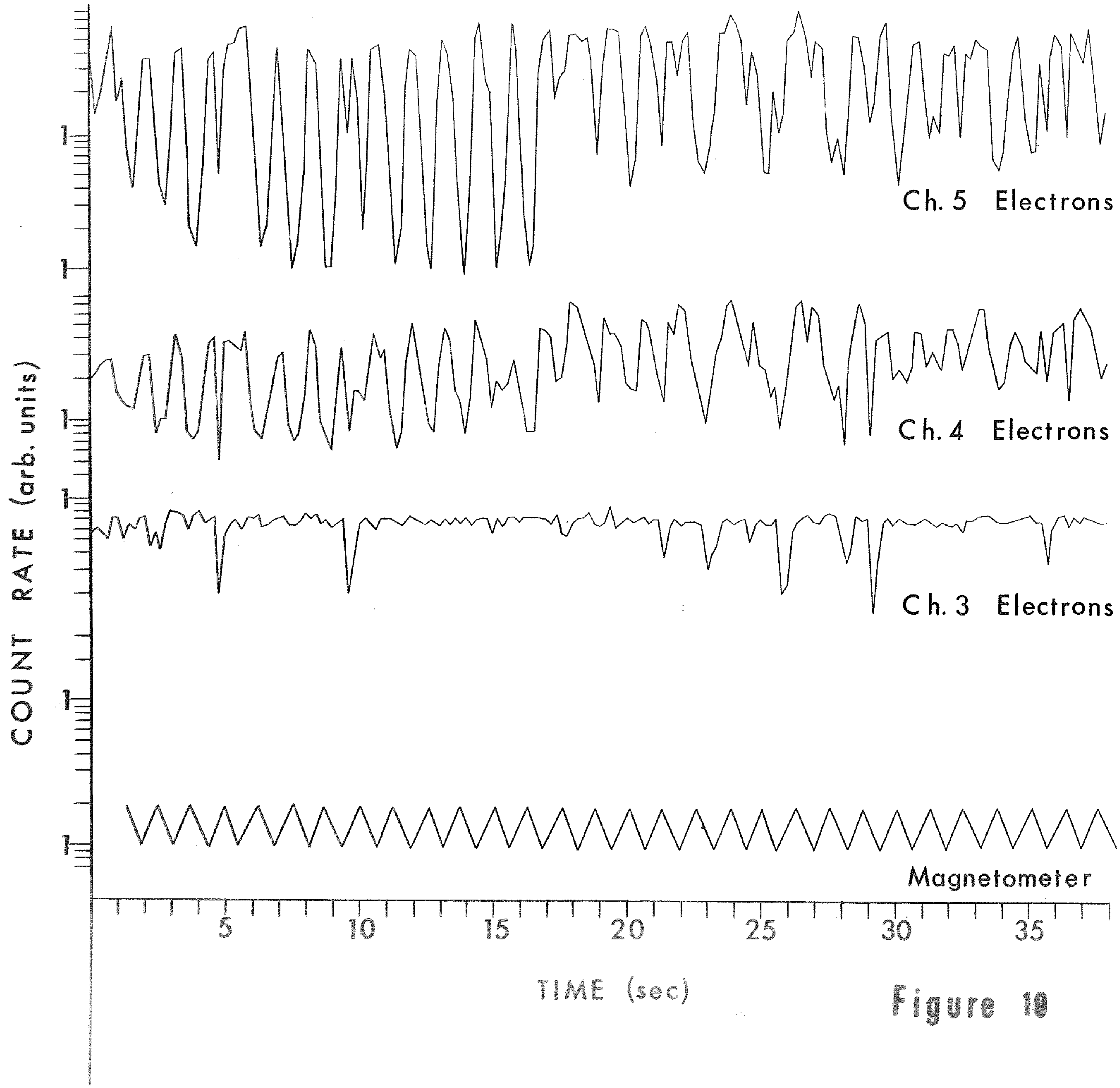
COUNT RATE (arb. units)
Ch. 5 Electrons
Ch. 4 Electrons
Ch. 3 Electrons
Magnetometer
5
10
15
20
25
30
35
TIME (sec)

Figure 10